Histone H3 K79 methylation states play distinct roles in UV-induced sister chromatid exchange and cell cycle checkpoint arrest in *Saccharomyces cerevisiae*

Alyssa A. Rossodivita, Anna L. Boudoures, Jonathan P. Mecoli, Elizabeth M. Steenkiste, Andrea L. Karl, Eudora M. Vines, Arron M. Cole, Megan R. Ansbro and Jeffrey S. Thompson[*]

Department of Biology, Denison University, Granville, OH 43023, USA

ABSTRACT

Histone post-translational modifications have been shown to contribute to DNA damage repair. Prior studies have suggested that specific H3K79 methylation states play distinct roles in the response to UV-induced DNA damage. To evaluate these observations, we examined the effect of altered H3K79 methylation patterns on UV-induced G1/S checkpoint response and sister chromatid exchange (SCE). We found that the di- and trimethylated states both contribute to activation of the G1/S checkpoint to varying degrees, depending on the synchronization method, although methylation is not required for checkpoint in response to high levels of UV damage. In contrast, UV-induced SCE is largely a product of the trimethylated state, which influences the usage of gene conversion versus popout mechanisms. Regulation of H3K79 methylation by H2BK123 ubiquitylation is important for both checkpoint function and SCE. H3K79 methylation is not required for the repair of double-stranded breaks caused by transient HO endonuclease expression, but does play a modest role in survival from continuous exposure. The overall results provide evidence for the participation of H3K79 methylation in UV-induced recombination repair and checkpoint activation, and further indicate that the di- and trimethylation states play distinct roles in these DNA damage response pathways.

INTRODUCTION

DNA is constantly subject to damage by external environmental forces and internal cellular activities (1). Different agents cause distinct forms of DNA damage. For example, ionizing radiation (IR) creates double-strand breaks in the DNA (2), and ultraviolet (UV) radiation causes the formation of cyclo-butane pyrimidine dimers (CPDs) and 6–4 photoproducts (3). DNA damage can pose a risk for the survival of cells through the inhibition of DNA replication or transcription, as well as undermining the integrity of genetic inheritance (2). The ubiquity of UV radiation and its effects on DNA results in it being one of the major causes of environmentally derived cancer in humans (4).

Cells possess a diverse array of DNA repair mechanisms to cope with and repair DNA damage. Damage inflicted by UV radiation is processed by three distinct repair pathways: nucleotide excision repair (NER), homologous recombination repair (HRR) and post-replication repair (PRR). NER is the primary means for the removal of CPDs incurred by UV, excising stretches of DNA containing bulky adducts/crosslinks, followed by synthesis of a new strand of nucleotides to fill the gap (5). Alternatively, cells may utilize damage tolerance mechanisms in the presence of high levels of damage and/or at critical times in the cell cycle. For example, while HRR is primarily implemented in the repair of double-stranded breaks, it is thought to serve as a bypass mechanism for UV damage that utilizes undamaged DNA strands as a template for replicating the missing or damaged portion (2,6,7). Similarly, PRR operates as a bypass mechanism for UV damage, relying in part on damage-tolerant DNA polymerases to complete unreplicated gaps on the damaged chromatid during DNA replication (8). The

[*]To whom correspondence should be addressed. Tel: +1 740 587 5581; Fax: +1 740 587 5634; Email: thompsonjs@denison.edu
Present address:
Alyssa A. Rossodivita, Timmy Global Health, 22 E. 22nd St., Indianapolis, IN 46202, USA.
Anna L. Boudoures, Division of Biology and Biomedical Sciences, Washington University in St. Louis, Campus Box 8226, 660 S. Euclid Ave, St. Louis, MO 63108, USA.
Jonathan P. Mecoli, Wisconsin Alumni Research Foundation, 614 Walnut Street, 13th Floor, Madison, WI 53726, USA.
Eudora M. Vines, University of Louisville School of Dentistry, 501 S. Preston, Louisville, KY 40202, USA.
Arron M. Cole, Anatomy and Cell Biology, University of Illinois at Chicago, 808 S. Wood St., Chicago, IL 60612-7308, USA.
Megan R. Ansbro, University of California, Irvine School of Medicine, 1001 Health Sciences Road, Irvine, CA 92697-3950, USA.

mechanism by which these various pathways are coordinately regulated is an area of active investigation.

The signaling of DNA damage and coordination of repair processes in eukaryotic organisms takes place within the context of chromatin, with histone proteins and their post-translational modifications contributing to these efforts. One of the best studied DNA-damage-associated histone modifications is phosphorylation of histone variant H2AX, which influences the accessibility at the break and recruitment of damage checkpoint and repair factors in higher eukaryotes (9,10). H3 lysine 79 (H3K79) methylation has also been implicated in DNA repair. From work done in the yeast *Saccharomyces cerevisiae*, it has been shown that loss of H3K79 methylation results in hypersensitivity to UV damage (11,12), while causing increased resistance to damage by methyl methanesulfonate (13). H3K79 methylation is required for UV- and IR-induced arrest at the G1/S and intra-S damage checkpoints, potentially serving as a binding site for checkpoint factor Rad9 (14–19). This modification also contributes to NER activity following UV exposure (20–22). Genetic analyses have further suggested a role for this modification in the context of recombination repair of IR and UV damage (11,12,23), and it has been shown that H3K79 methylation is important for chromatid cohesion and DNA resection during double-stranded break repair (24). But the role of H3K79 methylation in UV-induced recombination repair has not been evaluated.

H3K79 methylation exists in a number of specific 'states', and prior work from our lab suggests that these states possess distinct characteristics with respect to UV repair. H3K79 is modified by the histone methyltransferase Dot1 (25,26), which can add up to three methyl groups to a given H3K79 residue. H3K79 methylation state distribution is influenced by ubiquitylation of histone H2B lysine 123 by the ubiquitin conjugating/ligase pair Rad6 and Bre1 (27–29), which stimulates the production of the H3K79 trimethylated and possibly dimethylated states. Epistasis analysis of a collection of histone H3 substitution mutations that have unique effects on the distribution of H3K79 methylation states revealed that each of these mutations acts through a distinct subset of UV damage response and repair pathways (12), suggesting that there are distinct functions associated with each methylation state.

These prior analyses were done by quantifying survival following UV exposure, thus we wished to evaluate the relationship between H3K79 methylation states and UV damage in the context of specific DNA damage response and repair processes. We report here our examination of H3K79 methylation states with respect to UV-induced checkpoint arrest and sister chromatid exchange (SCE). The results presented here indicate that the role of H3K79 methylation in UV repair is exclusively a product of the di- and trimethylated states. Both states are important for UV-induced G1/S checkpoint arrest and SCE, but the relative importance of each state is distinct between these two processes.

MATERIALS AND METHODS

Yeast strains

Yeast strains used in this study are shown in Table 1. Deletion of the *DOT1* and *BAR1* genes in various strain backgrounds was done by polymerase chain reaction (PCR) mediated gene disruption, using the KanMX and *TRP1* disruption markers, respectively. Replacement of the wild-type gene encoding histone H3 (*HHT2*) with various mutant alleles of H3 was done by a plasmid swapping method, as previously described (12). The *RAD5* and *RAD52* genes were deleted in this background using plasmids pBJ22 (30) and pSM22 (provided by D. Schild), respectively. All deletions were confirmed by PCR. nullnull

To create strains lacking *BRE1*, the *URA3* locus was deleted in the parent strain by transformation with a PCR-generated copy of the *ura3Δ0* allele from BY4741. Transformants were selected on SD complete media containing 5-fluoroorotic acid. Deletion of the *URA3* locus was confirmed by PCR. *BRE1* was deleted in the resultant strain by PCR-mediated gene disruption (31), using *URA3* as the disruption marker, and was subsequently confirmed by PCR.

Strains were constructed to examine SCE using a previously described direct repeat reporter construct (32). Parent strain JTY34 was transformed with a PCR-generated copy of the *ADE2* gene from strain BY4741 to convert it to ADE+. Conversion of the *ADE2* locus was confirmed by PCR and DNA sequencing. The resultant strain (JTY34A1) was then transformed with a linearized copy of plasmid pLS189 to create JTY34ATA. Appropriate integration of the *ade2-n::TRP1::ade2-I* at the *ADE2* locus was confirmed by Southern blot. This strain was subsequently used to create other comparable reporter strains with varying mutations included, as described above.

UV survival assays

UV survival assays were done using mid-log phase cultures as previously described (11). UV exposures were done using a Philips 30W G30T8 UV lamp at 254 nm. Plates were incubated in complete darkness to prevent photoactivated repair. All assays were repeated a minimum of three times, and are reported as means $\pm$ 1 S.E.

UV checkpoint budding assays

To synchronize cells, cultures were grown overnight to early log phase (OD$_{600}$ = 1.0) in YEPD broth. Cultures were diluted to an OD$_{600}$ of ~0.2–0.3 in 1 ml of fresh YEPD containing *S. cerevisiae* α-factor at 15–30 μg/ml, and were incubated at 30°C for 3 h. Culture synchronization was verified microscopically by the presence of the 'shmoo' morphology in greater than 95% of the culture. Cultures were centrifuged, washed with cold sterile water, and resuspended in ~3.5 ml of ice-cold water. A 3 ml aliquot was stirred on a rotary shaker in 60 mm Petri dishes and irradiated with a Philips 30W G30T8 UV lamp at 254 nm. UV dosage was determined with a UVX Radiometer (UVP, Inc.). An appropriate volume of 10X YEPD was added to aliquots of the exposed and unexposed cultures, followed by incubation at 30°C in complete darkness. Aliquots of both cultures were collected every 15 min over a period of several hours, and examined microscopically for cell bud morphology. Mother cells with buds less than one-third their size were defined as 'budding cells' (33). A minimum of 100 cells were counted for each sample, and the percentage of

Table 1. *Saccharomyces cerevisiae* strains used in this study

Strain name	Genotype	Source
JTY34	*MAT a ade2–101 his3Δ200 lys2–801 trp1Δ901 ura3–52 hht1,hhf1::LEU2 hht2,hhf2::HIS3* plus pJT34 (*HHT2-HHF2 LYS2 CEN4 ARS1*)	(48)
JTY106	Isogenic to JTY34 except with pMS106 (*hht2-Q76R LYS2 CEN4 ARS1*)	(49)
JTY307	Isogenic to JTY34 except with pJTH3–7 (*hht2-T80A LYS2 CEN4 ARS1*)	(49)
JTY309	Isogenic to JTY34 except with pJT309 (*hht2-L70S LYS2 CEN4 ARS1*)	(49)
JTY34D	Isogenic to JTY34 except *dot1::kanMX4*	(11)
JTY106D	Isogenic to JTY34D except with pMS106 (*hht2-Q76R LYS2 CEN4 ARS1*)	(12)
JTY309D	Isogenic to JTY34D except with pJT309 (*hht2-L70S LYS2 CEN4 ARS1*)	(12)
AAY34r9	Isogenic to JTY34 except *rad9::URA3*	(11)
JTY34r52	Isogenic to JTY34 except *rad52::URA3*	(11)
JTY34A1	Isogenic to JTY34 except *ADE2*	This study
JTY34ATA	Isogenic to JTY34A1 except *ade2-n::TRP1::ade2-I*	This study
JTY106ATA	Isogenic to JTYA1 except with pMS106 (*hht2-Q76R LYS2 CEN4 ARS1*) and *ade2-n::TRP1::ade2-I*	This study
JTY307ATA	Isogenic to JTY34A1 except with pJTH3–7 (*hht2-T80A LYS2 CEN4 ARS1*) and *ade2-n::TRP1::ade2-I*	This study
JTY309ATA	Isogenic to JTY309 except with pJT309 (*hht2-L70S LYS2 CEN4 ARS1*) and *ade2-n::TRP1::ade2-I*	This study
JTY34DATA	Isogenic to JTY34ATA except *dot1::kanMX4*	This study
JTY106DATA	Isogenic to JTY106ATA except *dot1::kanMX4*	This study
JTY307DATA	Isogenic to JTY307ATA except *dot1::kanMX4*	This study
ABY34u0	Isogenic to JTY34 except *ura3Δ0*	This study
ABY34D	Isogenic to ABY34u0 except *dot1::kanMX4*	This study
ABY34br1	Isogenic to ABY34u0 except *bre1::URA3*	This study
ABY34Dbr1	Isogenic to ABY34br1 except *dot1::kanMX4*	This study
ABY106br1	Isogenic to ABY34br1 except with pMS106 (*hht2-Q76R LYS2 CEN4 ARS1*)	This study
ABY307br1	Isogenic to ABY34br1 except with pJTH3–7 (*hht2-T80A LYS2 CEN4 ARS1*)	This study
ABY34ATAu0	Isogenic to JTY34A1 except *ura3Δ0* and *ade2-n::TRP1::ade2-I*	This study
ABY34DATA	Isogenic to ABY34ATAu0 except *dot1::kanMX4*	This study
ABY34ATAbr1	Isogenic to ABY34ATAu0 except *bre1::URA3*	This study
ABY34DATAbr1	Isogenic to ABY34ATAbr1 except *dot1::kanMX4*	This study
DVY34ATAr5	Isogenic to ABY34ATAu0 except *rad5::URA3*	This study
DVY34DATAr5	Isogenic to ABY34DATA except *rad5::URA3*	This study
TSY34ATAr52	Isogenic to ABY34ATAu0 except *rad52::URA3*	This study
TSY34DATAr52	Isogenic to ABY34DATA except *rad52::URA3*	This study
JTY34b1	Isogenic to JTY34 except *bar1::TRP1*	This study
JTY106b1	Isogenic to JTY106 except *bar1::TRP1*	This study
JTY309b1	Isogenic to JTY309 except *bar1::TRP1*	This study
JTY34br1b1	Isogenic to ABY34br1 except *bar1::TRP1*	This study

budded cells was calculated. Checkpoint delay times were calculated from each trial as the difference in time at which the culture achieves 20% budding in UV-exposed relative to unexposed cells (15% was used for *bre1* strain in stationary phase due to lower budding frequency). Average times for each strain were compared by a one-way analysis of variance (ANOVA) with Dunnett's post-hoc test.

Comparable experiments were done by growing cultures into early stationary phase (36–48 h incubation, density $\geq 3 \times 10^8$ cells/ml). Culture synchronization was verified microscopically by the presence of single unbudded cells in more than 95% of the culture. UV-irradiation and microscopic evaluation was performed as described above, without the inclusion of α-factor.

UV-induced sister chromatid recombination assays

Strains possessing the *ade2-n::TRP1::ade2-I* SCE reporter construct were appropriately diluted and plated on YEPD agar in order to generate individual colonies. After two days of growth at 30°C, one red-colored colony from each strain, approximately 1 mm in size, was excised by cutting the area around each colony with a sterilized spatula and resuspending it in a microcentrifuge tube with sterile water

(in the case of experiments done with the *rad5* and *rad52* strains, 10 total colonies were resuspended in order to compensate for the lower UV survival frequency). The suspension was serially diluted and plated at appropriate concentrations onto YEPD and SD-ade plates (in duplicate for each). Plates were exposed to varying dosages of UV with a Philips 30W G30T8 UV lamp; dosages were calculated using a UVX Radiometer (UVP, Inc.). UV dosages used for each concurrently tested strain set were selected to result in a general survival frequency of ∼1–10% for the highest dosage employed. Plates were incubated for 3–4 days at 30°C in complete darkness. Viable colonies were counted, which was used to calculate the frequency of total recombination events relative to the survival frequency. Colonies from the SD-ade plates were then replica plated onto SD-trp plates, and incubated for an additional two days at 30°C, followed by counting the number of colonies on the SD-trp replicas. The number of ADE+TRP+ colonies was used to calculate the frequency of gene conversion events per viable cells, while the number of ADE+trp− colonies was used to calculate popout events per viable cells. Each strain was tested a minimum of five times. Averages for each strain were compared at each dosage by a one-way ANOVA with Tukey HSD post-hoc test.

Spontaneous sister chromatid recombination assays

Nine colonies from each strain (following ∼48 h of growth on plates, as described above), each approximately 1 mm in size, were excised from the plate with a sterilized spatula and resuspended in separate microcentrifuge tubes with sterile water. The suspensions were serially diluted, and proper dilutions of each culture were plated, in duplicate, onto YEPD and SD-ade plates, which were incubated at 30°C for 3–4 days. Colonies were counted, and ADE+ colonies were subsequently replica plated onto SD-trp plates, and counted after incubation at 30°C for two days. Rates for spontaneous sister chromatid gene conversion and popout events were calculated using the method of the median (34,35). Reported values are the mean of at least three assays per strain. Averages for each strain were compared by a one-way ANOVA with Tukey HSD post-hoc test.

Western blot analysis of histone H3K79 methylation levels

Yeast cultures (100 ml YEPD) were grown overnight either to log phase (Figure 7), to log phase followed by arrest with α-factor (0.5 µg/µl, using *bar1*- strains; Figure 3), or to stationary phase (Figure 3). Cultures were washed and resuspended in sterile chilled water, dispensed into 150 mm Petri dishes (30 ml maximum per dish), and exposed to the desired dosage of UV (indicated in corresponding figure legends). Appropriate volumes of 10X YEPD were added to exposed cultures (or unexposed controls), which were incubated shaking in complete darkness at 30°C for the indicated time; protease XIV (0.1 µg/µl) was included for cultures that were α-factor arrested. Following incubation, samples were incubated on ice with an equal volume of absolute ethanol, followed by a wash with sterile water prior to storage at −80°C. Nuclear protein extracts were isolated from the collected samples, as previously described (12,36). Nuclear pellets were resuspended in ∼200–300 µl of 1X Laemmli buffer containing 6 M urea and 4% β-mercaptoethanol. Equal amounts of protein were run on Any kD Mini-PROTEAN TGX gels (Bio-Rad) and transferred to PVDF membranes with a Trans-Blot Turbo Transfer System (BioRad). Blots were incubated with primary antibodies overnight at 4°C in TBS-Tween (0.05%) with 5% BSA at the indicated dilution (anti-H3, 1:15 000, Abcam #1791; anti-H3 K79me1, 1:500, Abcam #2886; anti-H3 K79me2, 1:3000, Cell Signaling Technology #5427; anti-H3 K79me3, 1:15 000, Cell Signaling Technology #4260). Blots were washed with TBS-Tween (0.05%) and subsequently incubated with anti-rabbit IgG-HRP antibody (1:3000 dilution, Millipore #12-348). Blots were washed again with TBS-Tween (0.3%, 0.1% and 0.05%, sequentially) and then developed using the ECL2 Western Blotting Substrate (Thermo Scientific) on a FluorChem HD2 Chemiluminescent Workstation (Alpha Innotech).

Densitometry of western blots was done to calculate relative changes in H3K79 methylation using AlphaEase FC Software (Alpha Innotech). Intensities of bands corresponding to histone H3 were measured, with background deducted using lane-specific background measurements. Intensities of bands for specific H3K79 methylation states were adjusted relative to the intensity of the bands detected by the general anti-H3 antibody to correct for minor loading variations. Intensities were further adjusted by deducting the intensity of bands associated with non-specific antibody binding observed in the *dot1*- strain. Intensities for specific strains and methylation states were subsequently normalized relative to the unexposed wild-type strain and corresponding methylation state to indicate relative methylation levels for each strain/exposure condition. Each culture growth/UV exposure/nuclei prep experiment was repeated at least five times for each of the conditions examined. Each set of nuclei preps was run on two sets of gels, and densitometry values of the two runs were averaged for each trial. Data from the separate trials were then averaged to generate the reported data. Results were statistically evaluated by Kruskal–Wallis one-way non-parametric analysis.

Spot-plate assays with HO-induced DNA damage

Strains to be tested were transformed with the plasmid pGAL-HO-pRS412 (37), possessing a galactose-inducible version of the gene encoding the HO endonuclease. For limited duration induction of endonuclease expression, transformed colonies were inoculated in selectable broth containing glucose, and allowed to grow for 24–48 h at 30°C. Cultures were then pelleted, washed in sterile water, with half of each culture resuspended in glucose selectable media, and the other half resuspended in galactose-containing selectable media, followed by incubation at 30°C for a specified length of time (4–28 h). Cultures were then pelleted, washed in sterile water, and resuspended at an OD_{600} of 1.0. Both the galactose-exposed and galactose-unexposed suspensions were serially diluted in 10-fold increments in a 96-well microtiter plate to a dilution of 10^{-4}. Five microliters of each dilution were spot-plated onto selectable media containing glucose in duplicate. Plates were incubated over a period of ∼7 days and photographed at various times during the incubation. Each strain was tested a minimum of three times, and photographs shown represent typical observations.

For assays examining continuous exposure to the HO endonuclease, plasmid-transformed colonies were inoculated in selectable broth containing glucose and allowed to grow for 24–48 h at 30°C. Each culture was diluted to an OD_{600} of 1.0 and serially diluted as described above. Five microliters of each dilution were spot-plated onto glucose- and galactose-containing selectable media in duplicate. Plates were incubated over a period of ∼7 days and photographed at various times during the incubation. Each strain was tested a minimum of three times, and photographs shown represent typical observations.

Hydroxyurea sensitivity

Colonies of strains to be tested were inoculated in YEPD broth and grown overnight at 30°C. Each culture was diluted to an OD_{600} of 1.0, and subsequently serially diluted in a 96-well microtiter plate to a dilution of 10^{-4}. Five microliters of each dilution were spot-plated onto SD complete plates containing or lacking hydroxyurea (200 mM) in duplicate. Plates were incubated over a period of ∼7 days and photographed at various times during the incubation.

Each strain was tested a minimum of three times, and photographs shown represent typical observations.

RESULTS

Histone H2B K123 ubiquitylation and H3 K79 methylation act in concert in response to UV damage

It has been previously shown by our group and others that histone H3K79 methylation is important with respect to UV damage response. Yeast cells lacking Dot1, the H3K79 methyltransferase, are hypersensitive to UV relative to wild-type cells (11), display defects in the G1/S DNA damage checkpoint (14–16), and have reduced nucleotide excision repair (20,21). Histone H2B K123 ubiquitylation is also important for the response to UV, as cells lacking this modification similarly possess G1/S checkpoint deficiencies (14–16). These two modifications are functionally related, as H2B ubiquitylation influences the levels of H3K79 methylation states. Our prior work suggests that H3K79 methylation states play distinct roles in the context of UV repair (12), and the effects of H2B ubiquitylation on H3K79 methylation may represent part of the mechanism by which these roles are regulated. But to date, the nature of this interaction and the specific roles played by H3K79 methylation states in UV repair have not been examined.

To gain insight into the relationship between these two modifications in UV repair, we examined survival of cells following exposure to various UV dosages. Survival was measured in strains lacking Dot1, Bre1, or possessing point mutations in histone H3 which have been previously shown to variably affect the level of H3K79 methylation (H3T80A, reduced K79me3; H3Q76R, reduced K79me2 and K79me3; both mutations increase K79me1; (12)). Consistent with previous observations, the *dot1* and H3Q76R mutations cause survival to decrease ∼50-fold relative to the wild-type strain (Figure 1). The H3T80A mutation also causes a decrease in survival, but to a lesser extent (∼5–10-fold). We similarly observed that a null allele of *BRE1*, the histone H2B K123 ubiquitin ligase, resulted in hypersensitivity to UV comparable to that observed in the *dot1* and H3Q76R strains, indicating that both modifications are involved in the response to UV damage.

Double mutant strains were examined to evaluate the genetic relationship between these modifications in UV repair. We observed that combining *bre1* with either the *dot1* or H3 mutations resulted in UV sensitivity comparable to that of the *bre1* single mutant strain (Figure 1). The *dot1 bre1* double mutant was somewhat more UV sensitive than either single mutant, although less so than would be expected for a fully additive phenotype. The *bre1* T80A and *bre1* Q76R double mutants were phenotypically indistinguishable from the *bre1* single mutant. The overall epistatic relationship between these mutations is consistent with the interpretation that H3K79 methylation and H2BK123 ubiquitylation act through a common genetic pathway following UV exposure, but the additivity observed in the *dot1 bre1* double mutant indicates that each modification has additional non-overlapping roles in UV repair.

Histone H3K79 di- and trimethylation contribute to UV-induced G1/S checkpoint arrest

It has been previously shown that methylation of histone H3K79 and H2BK123 ubiquitylation are required for the G1/S and intra-S checkpoint response in response to UV- and IR-induced DNA damage (14–19). Consistent with this observation, we have previously shown that mutations that alter or prevent H3K79 methylation act within the same epistasis group as checkpoint factor Rad9 (11,12). Given the previously established influence of H2BK123 ubiquitylation on H3K79 methylation, it would be predicted that the H3K79 di- and/or trimethylation levels would be specifically required for the DNA damage checkpoint response.

To evaluate the K79 methylation state specificity in UV-induced G1/S cell cycle arrest, we examined the effect of the aforementioned mutations in histone H3 that alter the distribution of K79 methylation levels on cell cycle progression following UV exposure. Logarithmically growing yeast cultures were arrested with α-factor, exposed to UV radiation, released from the α-factor arrest, and then monitored for emergence of buds over time. Bud emergence in baker's yeast is tightly associated with the onset of DNA replication, and thus can be used as an indicator of progression into S phase (33).

Wild-type cells exposed to 50 J/m² of UV exhibited a delay in the emergence of buds relative to unexposed control cells (∼25 minutes at 20% budded cells), indicating checkpoint activation in response to UV (Figure 2A, Table 2). In contrast, and consistent with previous observations (15), we found that the *dot1* and H3Q76R strains exhibited no UV-induced delay in bud emergence compared with unexposed cells, comparable to the absence of delay found in the checkpoint-defective *rad9* strain, indicating that reduction or loss of K79 methylation levels disrupt checkpoint activation. In contrast, the H3L70S mutation, which has been previously shown to cause an increase in H3K79 methylation (12), has a normal checkpoint response. Comparable to *dot1*, the *bre1* mutant strain exhibited minimal checkpoint delay (Figure 2B), consistent with prior reports that H2BK123 ubiquitylation is required for checkpoint activation (15,16). nullnull

The H3T80A mutation causes insensitivity to α-factor, thus we tested this mutation in cells arrested by growth into early stationary phase. Cultures were grown until predominantly populated by single unbudded cells that synchronously re-enter the cell cycle within ∼2 h following inoculation into fresh media (Figure 2C, Table 2). Comparable to our observations with α-factor arrested cells, UV exposure resulted in a delayed bud emergence in wild-type cells (∼35 min), but not in *dot1*, *rad9* and H3Q76R strains. However, the T80A mutant strain exhibited a delayed bud emergence comparable to that observed in the wild-type strain. The *bre1* mutant strain exhibited a checkpoint response (Figure 2D), albeit statistically shorter than that observed in the wild-type strain, in contrast to the observations with α-factor arrested cells.

To correlate the checkpoint arrest phenotypes in these strains with H3K79 methylation levels, methylation was measured by western blot using the same conditions as used in the checkpoint assays. Consistent with our previously
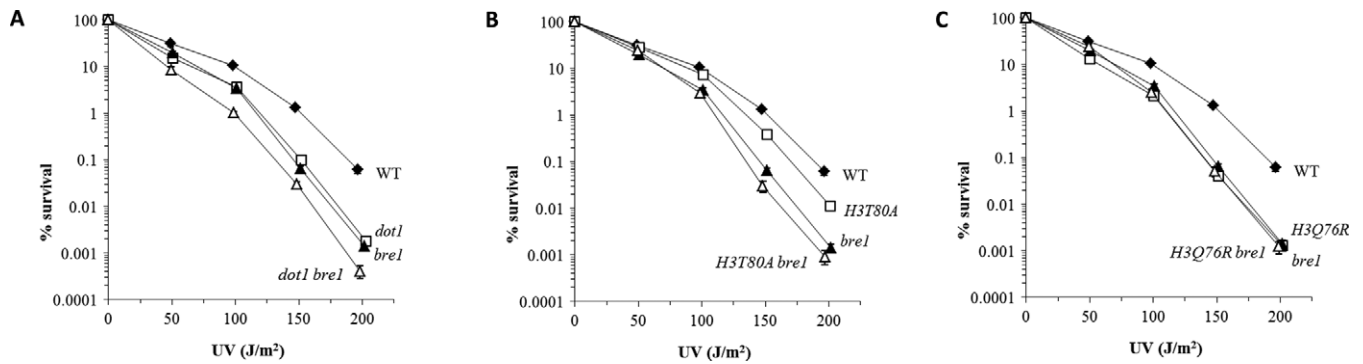
Figure 1. Epistasis analysis between *BRE1* and H3K79 methylation mutants. UV survival assays were done as described in the Materials and Methods section. Values are averages of at least three independent experiments; error bars represent one standard error. Strains used were (**A**) ABY34u0 (WT), ABY34D (*dot1*), ABY34br1 (*bre1*) and ABY34Dbr1 (*dot1 bre1*); (**B**) same as (A), except JTY307 (H3 T80A) and ABY307br1 (*h3T80A bre1*); (**C**) same as (A) except JTY106 (H3 Q76R) and ABY106br1 (H3 Q76R *bre1*).

Table 2. G1/S checkpoint delay times following UV exposure

Strain	Synchronization method	UV dosage (J/m^2)	Checkpoint delay (min)[a]
wild-type	α-factor	50	25.3 ± 2.6
dot1	α-factor	50	6.0 ± 2.2*
H3Q76R	α-factor	50	3.0 ± 2.7*
H3L70S	α-factor	50	26.0 ± 1.0
rad9	α-factor	50	1.3 ± 0.6*
wild-type	Stationary phase	50	35.0 ± 3.5
dot1	Stationary phase	50	2.3 ± 4.6*
H3Q76R	Stationary phase	50	4.3 ± 4.0*
H3T80A	Stationary phase	50	35.0 ± 7.3
rad9	Stationary phase	50	2.3 ± 5.0*
wild-type	α-factor	50	15.2 ± 2.3
bre1	α-factor	50	5.8 ± 4.3*
wild-type	Stationary phase	50	40.0 ± 8.5
bre1	Stationary phase	50	27.3 ± 8.8*
wild-type	α-factor	100	46.1 ± 7.6
dot1	α-factor	100	47.0 ± 8.7
H3Q76R	α-factor	100	44.0 ± 7.6
rad9	α-factor	100	37.2 ± 5.8

[a]Checkpoint delay reflects the difference in time at which the culture achieves 20% budding in UV-exposed relative to unexposed cells (15% used for *bre1* strain in stationary phase due to reduced budding frequency). Values are means $\pm$ 1 S.D. *, significantly different from wild-type ($p < 0.01$, except *bre1* in stationary phase, $p < 0.05$).

published observations, the H3T80A mutation caused a substantial decrease in trimethylation, but had no effect on dimethylation, while the H3Q76R mutation caused a large decrease of both di- and trimethylated states (Figure 3). Both mutations also resulted in an increase in monomethylation, while the H3L70S mutation caused increases in both mono- and dimethylation. The *bre1* mutation caused a nearly complete loss of H3K79 trimethylation and an increase in monomethylation, but had no impact on dimethylation. Relative methylation state levels for each strain varied slightly between α-factor and stationary phase arrested cells, but the general patterns were comparable in both conditions. Only minor differences were observed in pre- versus post-exposed cells, nearly all of which were statistically insignificant.

Comparing the relative methylation state levels in these strains with their checkpoint phenotypes, a correlation was observed between di- and trimethylation levels and relative checkpoint delay times (Figure 4), although the relative influence of these two methylation states on checkpoint arrest varied depending on the method of culture arrest. In

α-factor arrested cells, relative checkpoint delay time is correlated with trimethylation levels, while the correlation is stronger with the dimethylated state in stationary phase arrested cells. In contrast, no relationship was observed between checkpoint delay times and monomethylation levels. Overall, the results indicate that the di- and trimethylation states are variably required for UV-induced checkpoint activation, while the monomethylated state is insufficient.

Since the histone H3 mutations that affect K79 methylation levels exhibit their most pronounced effects on survival at higher UV dosages (12), we evaluated checkpoint response in cells exposed to elevated dosages of UV. In contrast to the checkpoint assays described above at 50 J/m^2, we found that checkpoint activation was not dependent on K79 methylation at 100 J/m^2. Wild-type, *dot1* and H3Q76R strains displayed UV-induced delayed bud emergence of ∼45 min, indicating normal checkpoint activation (Figure 5, Table 2). The *rad9* strain displayed a slightly shorter bud emergence delay (∼37 min), although the difference between this strain and the others was not statistically significant. Thus, checkpoint activation at higher dosages is
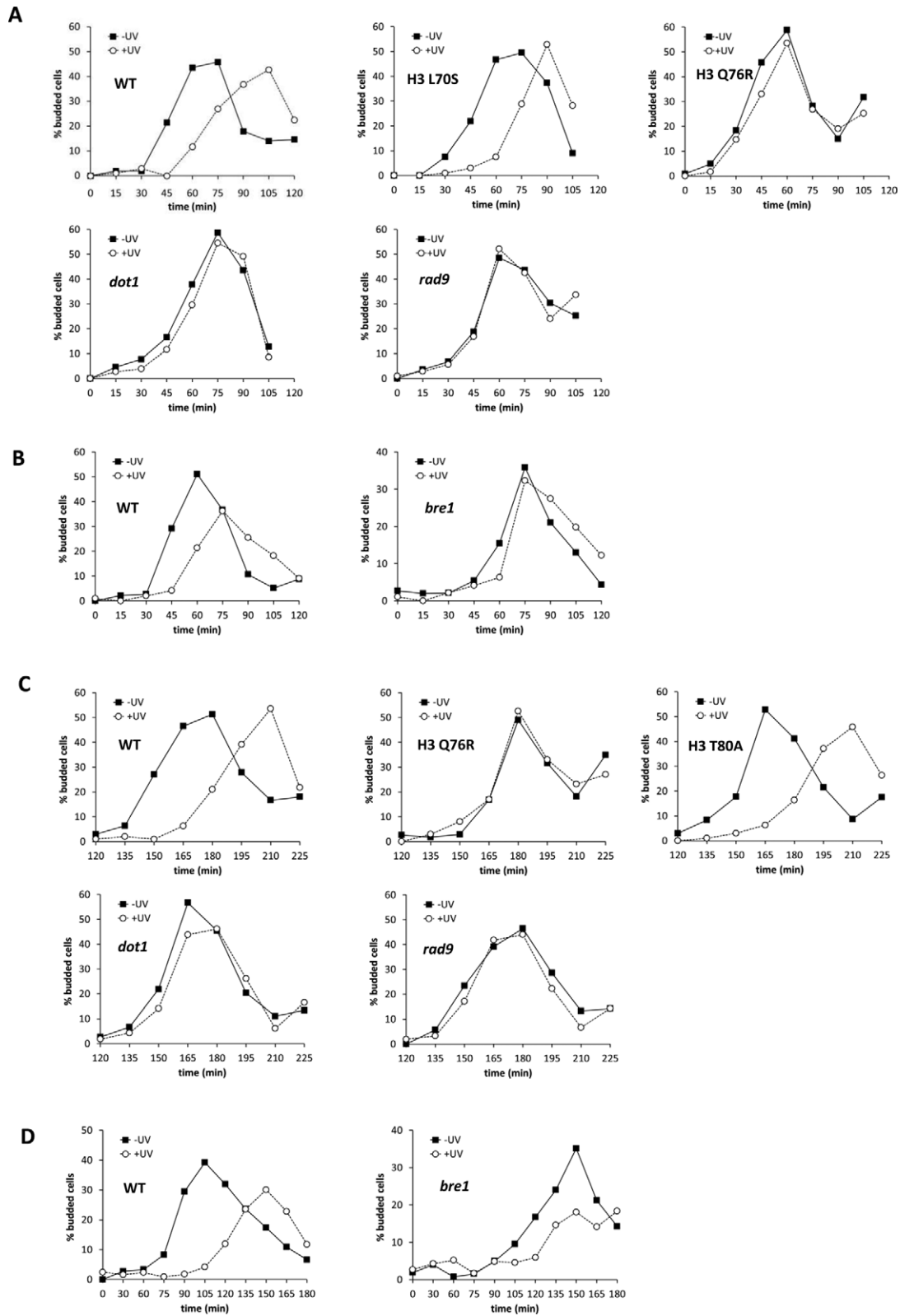
Figure 2. UV-induced G1/S checkpoint analysis of H3K79 methylation mutants. Strains were arrested with α-factor (**A** and **B**) or growth to stationary phase (**C** and **D**), and exposed to UV (50 J/m^2), and the frequency of small budded cells was measured over time, as described in the Materials and Methods section. Representative experiments are shown; quantitative compilation of data is displayed in Table 2. Strains utilized were (A and C) JTY34 (WT), JTY34D (*dot1*), JTY106 (H3 Q76R), JTY309 (H3 L70S) and AAY34r9 (*rad9*), and (B and D) ABY34u0 (WT) and ABY34br1 (*bre1*).
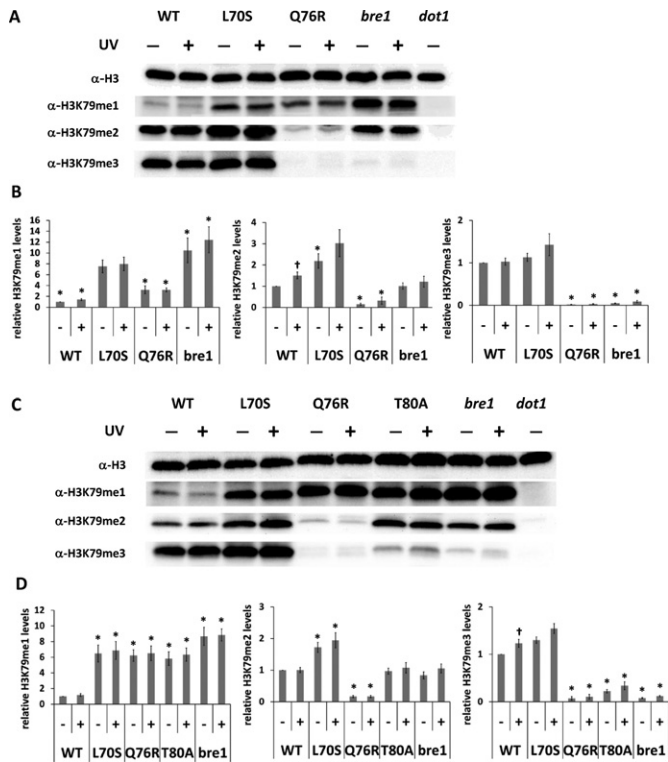
Figure 3. Western blot analysis of H3K79 methylation levels following UV exposure. Cultures were grown and arrested either with α-factor (**A**) or by growth into stationary phase (**C**), and exposed to UV, as in Figure 2. Strains used were the same as those in Figure 2, except also *bar1* in (**A**), in order to utilize lower concentrations of α-factor. Samples were collected 30 (**A**) or 60 (**C**) minutes after UV exposure. (**B** and **D**) Densitometry of H3K79me1, H3K79me2 and H3K79me3 levels from α-factor and stationary phase arrested cultures, respectively. Values represent mean of at least four independent exposures, normalized to the unexposed wild-type levels for each methylation state; error bars represent one standard error. *, significantly different from corresponding WT value ($p < 0.01$); †, significant difference between UV exposed and unexposed ($p < 0.01$).
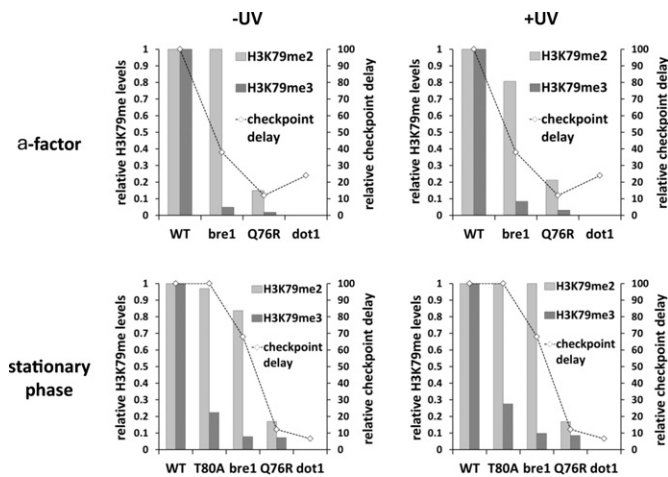

Figure 4. Correlation of H3K79 dimethylation and trimethylation levels relative to checkpoint delay time. Labels above and to the left of the graphs indicate the relevant conditions for each data set. K79 methylation levels from Figure 3 were normalized to WT levels for each methylation state on each graph. Checkpoint delay times from Table 2 were similarly normalized relative to WT levels, and are reported as percentages. Monomethylation levels were excluded to enable appropriate scaling of the relative methylation levels and checkpoint delays.
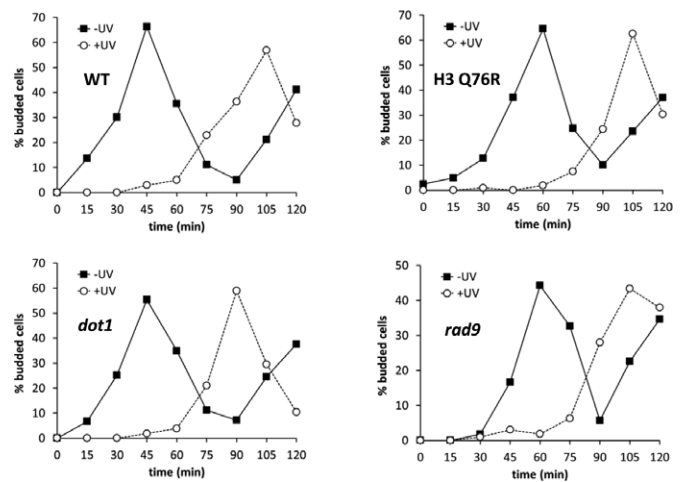

Figure 5. G1/S checkpoint analysis of H3K79 methylation mutants at 100 J/m². Conditions and strains used are as described in Figure 2.

not dependent on H3K79 methylation, and potentially utilizes a distinct mechanism from that initiated in response to lower UV dosages.

H3K79 trimethylation is primarily responsible for UV-induced sister chromatid exchange

Our prior epistasis analysis indicated a genetic overlap between H3K79 methylation and the *RAD52* epistasis group (11,12), which is involved in recombination repair. Recombination repair has been most extensively characterized in the repair of double-stranded breaks, but mutations in this epistasis group also cause sensitivity to other forms of DNA damage, including that caused by UV. While the precise role for recombination repair in response to UV damage remains an area of active investigation, it has been proposed that recombination could serve to repair breaks caused by UV-induced replication fork collapse (38). Alternatively, recombination could be utilized as a means of completing replication of UV-damaged templates via a 'template switching' process with the undamaged sister chromatid (7).

To evaluate a potential role for H3K79 methylation in SCE in response to UV damage, we utilized a previously designed reporter construct composed of two non-functional copies of the *ADE2* gene flanking a functional copy of the *TRP1* gene (Figure 6A; (32)). Each of the copies of *ADE2* possesses distinct mutations at their 3′ (*ade2-n*) and 5′ (*ade2-I*) ends, respectively. Unequal exchanges between the two alleles, either intra- or inter-chromosomally, result in the creation of a functional *ADE2* gene. Such events can occur through a gene conversion mechanism, leaving the intervening *TRP1* intact, or can occur via a 'popout' event, resulting in the deletion of the *TRP1* gene on the chromatid possessing the restored *ADE2* gene. Thus, by measuring the frequency of cells that are prototrophic for adenine and tryptophan synthesis, we can determine the frequency of these two classes of recombination events.

Strains possessing mutations that alter H3K79 methylation were exposed to UV and evaluated for the frequency of gene conversion and popout events in surviving cells.
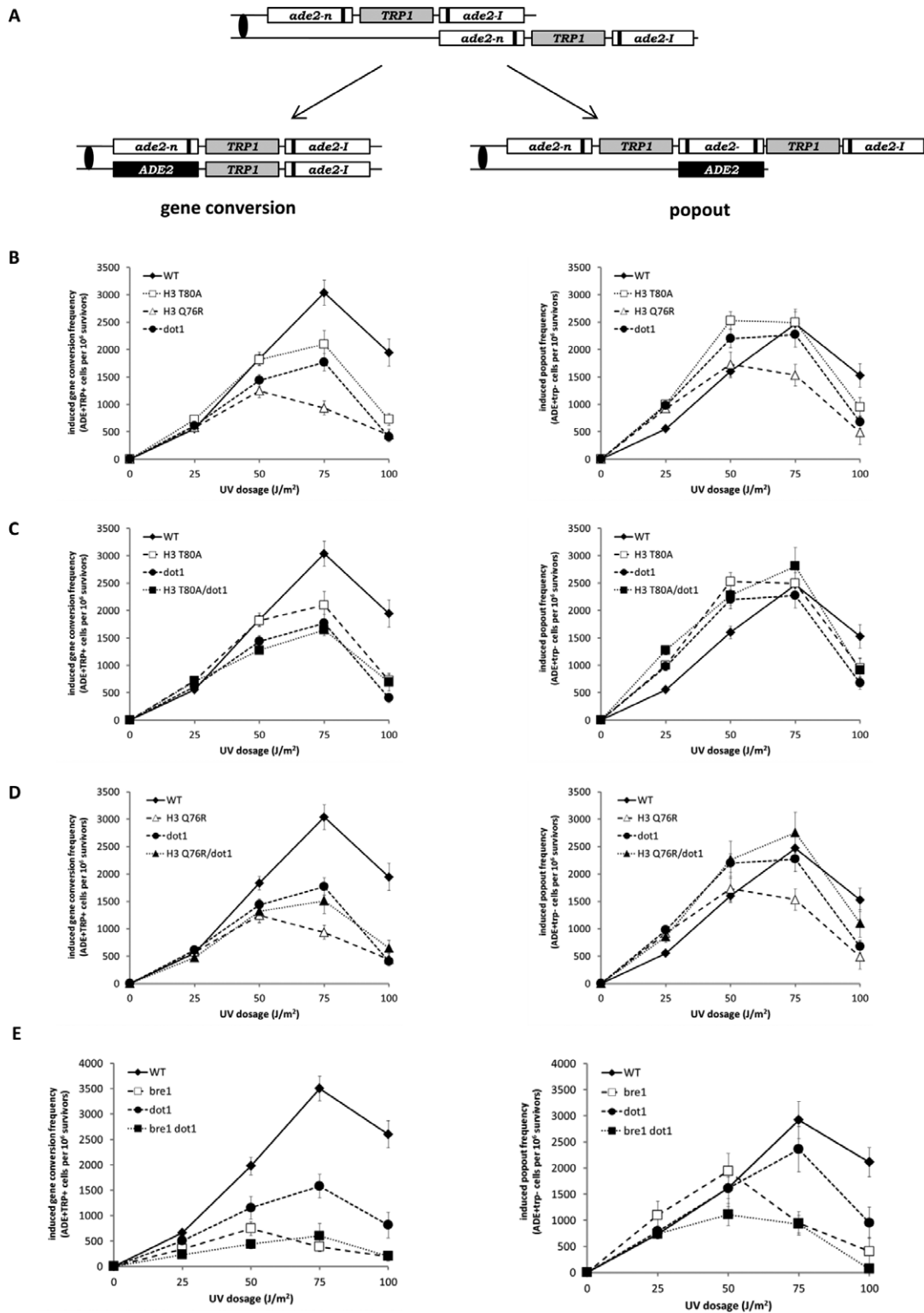
Figure 6. UV-induced sister chromatid exchange analysis of H3K79 methylation mutants. UV-induced SCE assays were performed as described in the Materials and Methods section. Values indicated are the number of cells of the indicated phenotype per 10^6 UV-surviving cells, reported as the mean of at least five independent experiments; error bars represent the standard error. Graphs on the left depict gene conversion frequencies, while those on the right represent popout frequencies. (**A**) Schematic depiction of the reporter construct used (32), and the potential recombination outcomes. The black vertical bars in the ade2-n and *ade2-I* boxes represent the relative position of the mutation in each respective allele. Interchromatid exchange outcomes are shown; intrachromatid exchanges are also possible, but not schematically shown. The bottom chromatid for each outcome (ADE+ TRP+ for gene conversion, ADE+ trp− for popout) represents the chromatid that is phenotypically detected in this assay. Strains used are as follows: (**B**) JTY34ATA (WT), JTY106ATA (H3 Q76R), JTY307ATA (H3 T80A), JTY34DATA (*dot1*); (**C**) same as (B) except JTY307DATA (H3T80A/*dot1*); (**D**) same as (B) except with JTY106DATA (H3 Q76R/*dot1*); (**E**) ABY34ATAu0 (WT), ABY34ATAbr1 (*bre1*), ABY34DATA (*dot1*) and ABY34DATAbr1 (*bre1 dot1*).
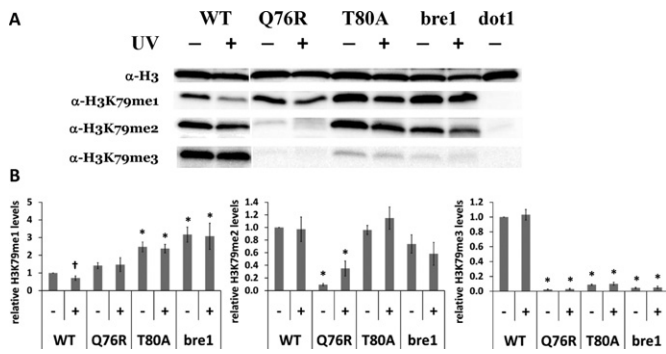
Figure 7. Western blot analysis of H4K79 methylation levels in log phase cultures. Cultures were grown in conditions comparable to those used for sister chromatid exchange assays in Figure 6, except that strains lacked the SCE reporter construct, to avoid mixed populations of ade− and ADE+ cells (which exhibit distinct growth kinetics). Suspended cultures were exposed to UV at 125 J/m^2 (corresponding to ∼75 J/m^2 for plate exposures, based on relative survival frequencies), and incubated for 1 h after exposure. Representative blots (**A**) and densitometry (**B**) are shown as described in Figure 3.
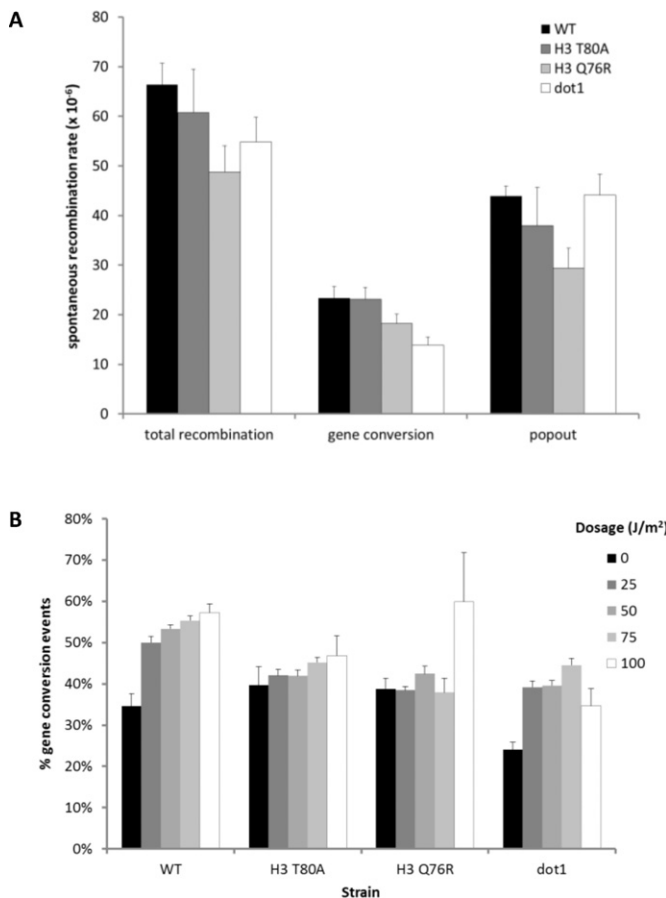

Figure 8. Spontaneous sister chromatid exchange analysis of H3K79 methylation mutants. (**A**) Spontaneous sister chromatid exchange rates were measured by the method of the median (34,35), using the SCE reporter strains listed in Figure 6, as described in the Materials and Methods section. Values reported are means of at least three independent experiments. Error bars represent the standard error. (**B**) Percentage of total SCE events (spontaneous for 0 J/m^2, UV induced for other dosages) that were categorized as gene conversion events. Data are calculated from experiments reported in Figures 6 and 8A.
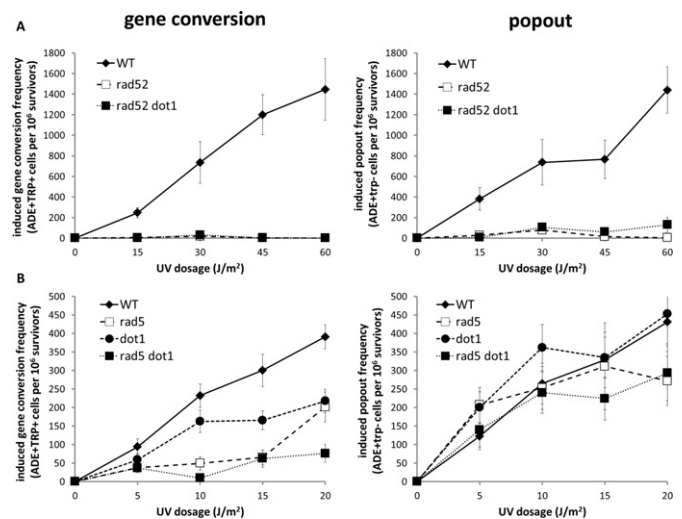

Figure 9. UV-induced sister chromatid exchange analysis of *BRE1*, *RAD5* and *RAD52* mutants. UV-induced SCE assays were done as described in the Materials and Methods section, and as depicted in Figure 6. Gene conversion events are shown on the left, and popout events on the right. Strains used are as follows: (**A**) JTY34ATA (WT), TSY34ATAr52 (*rad52*) and TSY34DATAr52 (*rad52 dot1*); (**B**) JTY34ATA (WT), DVY34ATAr5 (*rad5*), JTY34DATA (*dot1*) and DVY34DATAr52 (*rad5 dot1*).
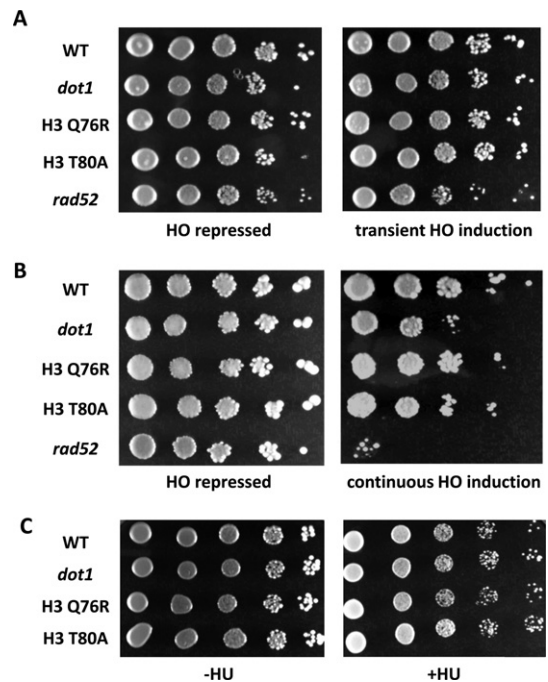

Figure 10. HO endonuclease and hydroxyurea sensitivity analysis of H3 K79 methylation mutants. (**A**) Strains were transformed with a plasmid possessing a galactose-inducible gene encoding for endonuclease HO. Cultures were grown in liquid media containing either glucose (HO repressed) or galactose (transient HO induction) for 4 h, followed by 10-fold serial diluting and spot plating on selectable media with glucose. Plates were photographed after ∼4 days of growth. Images shown are representative of the replicated experiments executed. Strains used: JTY34 (WT), JTY34D (*dot1*), JTY106 (H3 Q76R), JTY307 (H3 T80A) and JTY34r52 (*rad52*). (**B**) HO transformed strains listed in (A) were grown in selectable media with glucose overnight, followed by serial diluting and plating on selectable media containing either glucose (HO repressed) or galactose (continuous HO induction). (**C**) Overnight cultures were serially diluted 10-fold and spot-plated on YEPD plates lacking (−HU) or containing (+HU) hydroxyurea at 200 mM.

As previously reported with comparable reporter constructs (39,40), the frequency of recombination events increased in response to UV exposure (Figure 6B), reaching a maxima at ∼75 J/m². Increases were observed for both gene conversion and popout events, with gene conversion events being favored by a ∼3:2 ratio in wild-type cells. The H3T80A, H3Q76R and *dot1* mutations resulted in decreased UV-induced gene conversion events by ∼50–75% relative to the wild-type strain. There were some differences in the degree of reduced gene conversion between the three mutations examined, although most were not statistically significant (the lone exception being the lower levels exhibited by the H3Q76R mutation at 75 J/m²). In contrast, reduced K79 methylation levels resulted in a modest increase in popout events at lower UV dosages, followed by a small reduction at the highest dosage.

Epistasis analysis was done by comparing H3 and *dot1* mutations with corresponding double mutants. Double mutant strains displayed levels of UV-induced gene conversion and popout events comparable to that observed in the single mutant strains (Figure 6C and D), with no statistically significant differences between the single mutant strains and the corresponding double mutants. The genetic relationship between *dot1* and the H3 mutations indicates that the effects of the H3 mutations are within the same pathway as Dot1 in the context of UV-induced SCE, and is consistent with the influences of these mutations being a product of their effects on K79 methylation levels.

We also evaluated the potential role of H2BK123 ubiquitylation in UV-induced SCE in *bre1* strains. We found that the *bre1* mutation resulted in a significant reduction in UV-induced gene conversion events, and dosage-dependent changes to UV-induced popout events, somewhat more pronounced than that observed in the *dot1* mutant (Figure 6E). The *bre1 dot1* double mutant strain exhibited patterns comparable to the *bre1* mutant strain, indicating that the roles of H2BK123 ubiquitylation and H3K79 methylation in UV-induced SCE are through a common pathway.

To relate H3K79 methylation levels with UV-induced SCE activity, methylation levels in the various strains used in these assays were evaluated by western blot analysis using growth conditions equivalent to those used for the SCE assays. Comparable influences of the H3, *dot1* and *bre1* mutations on H3K79 methylation state levels were observed (Figure 7) relative to those described above in the checkpoint experiments. Almost no significant changes in methylation levels were observed in UV-exposed versus unexposed cells. Given the similarity in SCE phenotype and the commonality of reduced trimethylation in these mutant strains, this methylation state appears to be primarily responsible for the role of K79 methylation in UV-induced SCE.

To determine if the role of H3K79 methylation in SCE is specific to UV damage or plays a generalized role in recombination, we measured the rate of spontaneous SCE events by fluctuation analysis (34). For the most part, changes in K79 methylation did not affect spontaneous SCE (Figure 8A), regardless of the recombination mechanism. There were no statistically significant differences observed between the wild-type and H3 mutant strains, although the *dot1* mutant strain has a slightly lower rate of gene conver-

sion events. Thus, the role of K79 methylation in SCE is primarily in the context of UV-induced events.

These results also revealed that K79 methylation influences the proportion of gene conversion versus popout events that are induced by UV. Spontaneous SCEs were observed to favor popout events (∼2:1 ratio of popout-to-gene conversion). As noted above, this ratio was found to shift toward gene conversion events in response to UV exposure in wild-type cells in a dosage-dependent manner (Figure 8B). However, mutations affecting K79 methylation resulted in a distribution of UV-induced popout and gene conversion events comparable to the proportion observed in unexposed cells. Thus, K79 methylation is not only important for UV-induced SCE, but it also influences the mechanism by which these exchanges occur.

The exact mechanism of UV-induced SCE is not clear, but has been suggested to arise from a 'template-switching' mechanism, in which the fully replicated chromatid is temporarily utilized as a template in order to complete replication of gaps that result from UV-induced dimers in the other chromatid template (41). The process could occur through the usage of machinery that is part of the homologous recombination pathway represented by the *RAD52* epistasis group. But it has also been shown that the *RAD5* pathway, which operates as a part of the post-replication repair pathway (represented by the *RAD6* epistasis group), may also participate in this process. *RAD5* encodes for a SNF2/SWI2 family member ATPase with helicase activity, which has been proposed to mediate such a template-switching mechanism operating in parallel to the Rad52 pathway (7).

To determine if H3K79 methylation operates through either a *RAD52* and/or a *RAD5* dependent mechanism in the context of UV-induced SCE, we utilized the direct repeat reporter system described above. We observed that *rad52* mutants were completely defective for UV-induced SCE in both gene conversion and popout mechanisms. Virtually no increase in ADE+ prototrophs was identified from surviving cells following UV exposure (Figure 9A). Combining the *rad52* mutation with *dot1* had no effect on SCE frequencies. Thus, Rad52 is absolutely required for all UV-induced SCE events at this locus. In contrast, *rad5* mutants displayed reduced SCE exclusively with respect to gene conversion events (Figure 9B), with little to no effect on popouts. Double mutant strains lacking both *rad5* and *dot1* displayed a reduction in UV-induced gene conversion comparable to the *rad5* strain (with the exception of the highest UV dosage tested), suggesting that K79 methylation operates predominantly through a pathway involving Rad5 with respect to UV-induced SCE.

Loss of histone H3K79 methylation does not cause sensitivity to double-stranded breaks or hydroxyurea

As noted earlier, recombination processes may be utilized for the repair of double-stranded breaks caused by replication fork collapse in response to UV damage (38). It has been previously shown that loss of K79 methylation results in hypersensitivity to IR (23), suggesting that this modification is important for double-stranded break repair. However, conflicting reports have led to uncertainty as to

whether this modification is important for the checkpoint response to double-stranded breaks.

If the role of K79 methylation in UV-induced recombination repair is associated with double-stranded breaks that arise in response to stalled replication, we would expect that reduction or loss of K79 methylation would result in sensitivity to double-stranded breaks in general. To test this hypothesis, a double-stranded break was introduced in cells via the HO endonuclease. HO creates a lone double-stranded break at the yeast *MAT* locus, which can be repaired by homologous recombination with the HM loci, as part of a mating type switching mechanism (42). HO was introduced into strains under the control of the *GAL1-10* promoter, enabling regulated expression induced by exposure to galactose. Strains possessing various H3 or *dot1* mutations were grown in media containing galactose for limited periods of time (4–20 h), followed by plating on media containing glucose to repress HO expression. None of the histone or *dot1* mutant strains displayed any reduction in viability following growth in galactose (Figure 10A), indicating that repair of the HO induced break was not impaired. However, when cells were plated directly on galactose-containing media, some differences were observed (Figure 10B). The *dot1* strain displayed modest sensitivity to continuous HO expression, although much less so than observed in the *rad52* strain. However, neither of the H3 mutations tested resulted in any notable changes in viability. Thus, while complete loss of K79 methylation results in sensitivity to continuous induction of double-stranded breaks by HO, specific reduction of the K79 di- and/or trimethylated states does not result in any sensitivity.

UV damage can cause the collapse of replication forks as a result of slowed or impaired replication. To determine if the role of K79 methylation is associated with the response to slowed replication, we evaluated sensitivity of H3 and *dot1* mutations to hydroxyurea (HU), which causes slowed/stalled replication as a result of depleted nucleotide pools in the nucleus. While all strains tested displayed impaired growth in response to continuous exposure to HU relative to unexposed cells, none of the H3 or *dot1* mutations caused increased sensitivity to HU relative to the wild-type strain (Figure 10C). Thus, H3K79 methylation does not appear to serve as part of a general response to slow or impaired DNA replication.

DISCUSSION

We have presented evidence demonstrating that H3K79 methylation plays important roles in checkpoint response and SCE in response to exposure to UV radiation. While a role for this modification in checkpoint response and homologous recombination of double-stranded breaks has been previously reported, this is the first evidence implicating its role in UV-induced recombination repair. The data indicate that the functionality of K79 methylation in response to UV damage is largely undertaken by the di- and trimethylated states, and is dependent on ubiquitylation of histone H2BK123, consistent with prior work establishing a 'crosstalk' relationship between these two modifications. No specific function can be attributed to the H3K79 monomethylated state in UV repair, although the

partially additive phenotype in the *bre1 dot1* strain with respect to survival following UV exposure indicates that both of these genes have independent roles in UV repair. This could be due to unknown functions of H3K79 monomethylation, H2BK123 ubiquitylation itself, and/or the influence of H2BK123 ubiquitylation on H3K4 methylation in response to UV damage (20,43). We cannot rule out the possibility that the phenotypic effects reported here are due to alteration of other histone modifications by these H3 mutations. However, H3K79 methylation is not known to influence other histone modifications, and prior epistasis analysis suggests that the effects of these mutations are entirely due to their impact on K79 methylation (12).

While the di- and trimethylated states both contribute to UV repair, distinctions exist with respect to the relative importance of each methylation state to specific damage responses. In the context of UV-induced checkpoint activation, loss of di- and trimethylation, as caused by the Q76R mutation, results in complete loss of the G1/S checkpoint, indicating that the monomethylated state is insufficient on its own to initiate the response. In contrast, substantial reduction of trimethylation alone, as observed in the T80A mutant strain, has no impact on checkpoint activation. This suggests that either trimethylation is not required as long as dimethylation levels are unaffected, or that trimethylation levels at least $\sim$20–30% of wild-type are sufficient for function. The latter possibility is supported by the results from the *bre1* strain, which exclusively causes a nearly complete loss of the trimethylated state ($<$10% of wild-type levels; statistically lower than T80A, $p < 0.05$) and a partial reduction in relative checkpoint delay. However, the interpretation of the *bre1* results is complicated by the variable effect of this mutation on checkpoint delay depending on the manner by which cultures were grown and arrested (70% of WT checkpoint delay in α-factor arrest versus 40% in stationary phase arrest), and the possible influences of H2B ubiquitylation itself and/or its effect on H3K4 methylation on checkpoint activity. However, the fact that the *bre1* mutation does not cause a complete loss of checkpoint function indicates that checkpoint activation is not due to trimethylation alone. Therefore, these results indicate that the di- and trimethylated states both contribute to UV-induced G1/S checkpoint response to varying degrees, with the relative influence of each state in part dependent on the growth state of the cell. Further exploration into the mechanism by which H3K79 methylation participates in checkpoint activation will be needed to investigate whether these two states serve overlapping or distinct roles in this process.

Our results also revealed a dosage-dependent relationship between K79 methylation and UV-induced checkpoint response. While K79 methylation is clearly required for checkpoint response to UV at 50 J/m^2, this checkpoint is K79 methylation-independent at 100 J/m^2. Furthermore, we find that the checkpoint response is also partially functional in a Rad9-deficient strain at this dosage, indicating that higher levels of UV damage elicit a distinct Rad9-independent response, consistent with previous reports (44). These observations suggest that other mechanisms influence cell cycle progression depending on the degree of damage and/or the efficiency of repair during the checkpoint arrest (45).

In contrast to the roles for both K79 di- and trimethylation in checkpoint activation, the role for UV-induced SCE is largely a product of the trimethylated state. Reduced K79 methylation results in a substantial decrease in UV-induced gene conversion events (with relatively minimal effects on UV-induced popout events or spontaneous recombination events), and nearly all of the observed effect can be accounted for by the loss of the trimethylated state. Concomitant loss of dimethylation has little additional impact on SCE. The *bre1* mutation causes a greater reduction in UV-induced gene conversion compared to the H3 point mutations and the *dot1* mutation, indicating that ubiquitylation of H2BK123 plays an additional contributing role to this process beyond its effects on H3K79 methylation. It is possible that the primary role of the trimethylated state in UV-induced SCE is a result of the distribution of K79 methylation states at the *ADE2* locus (at which these events were measured), which is modestly enriched in trimethylated H3K79 (46). Further studies using reporter constructs at other loci will be needed to gain a comprehensive understanding of the role of H3K79 methylation states in UV-induced SCE.

Our analysis further indicates that the role of H3K79 methylation in SCE operates via a Rad5-dependent repair mechanism, potentially serving to influence the usage of a gene conversion mechanism. We find that UV-induced gene conversion events are favored over popouts at a ~3:2 ratio in our wild-type strain, while loss of H3K79 methylation results in an inverted ratio. We have previously demonstrated an epistatic relationship between *rad5* and *dot1* (as well as other H3 mutations) in the context of UV survival (11), and have further shown that loss of H3K79 methylation has no effect on UV-induced mutagenesis (11,12). Given that Rad5 represents an error-free branch of the post-replication repair pathway, these collective observations lead us to propose that H3K79 methylation either serves to promote Rad5-dependent gene conversion events, or conversely suppresses popout/crossover events. In this capacity, it may serve to guard against recombination events that are more prone to genetic alteration or loss. It is not clear how H3K79 methylation contributes to this process, although studies implicating this modification in the recruitment of cohesin to double-stranded breaks suggest that a comparable role in UV repair might exist (24).

In contrast to its role in UV-induced SCE, our observations suggest that the role of H3K79 methylation in DNA repair is not driven by stalled replication or double-stranded breaks. For the most part, mutations affecting H3K79 methylation did not cause sensitivity to hydroxyurea or HO-induced breaks. The lack of sensitivity to double-stranded breaks is consistent with a comparable observation reported previously (13), but contrasts with other reports of IR sensitivity in *dot1* strains (23,47). We cannot explain this inconsistency, other than to propose that IR-induced damage may be distinct from endonuclease inflicted breaks, or that there may be strain-specific differences present between these studies. We did observe differences in survival when cells were exposed to continuous expression of HO, suggesting that H3K79 methylation may influence how perpetual DNA damage is processed. But since this hypersensitivity was only observed in the complete absence of H3K79

methylation, it suggests that the role of this modification in UV repair is mechanistically distinct from that in double-stranded break repair.

The specific mechanisms by which H3K79 methylation participates in UV-induced checkpoint activation and SCE remain to be elucidated. While some evidence has been published implicating this modification as a binding site for DNA repair factors (17), it is not yet clear if this modification is a docking site for repair machinery, a regulator of repair gene transcription, a modulator of repair-specific chromatin structures, or another function that has yet to be elucidated. Whichever the case, the results presented here indicate that distinct H3K79 methylation states are not interchangeable, and must be factored into models addressing the role of this modification in DNA repair.

REFERENCES

1. Jackson,S.P. and Bartek,J. (2009) The DNA-damage response in human biology and disease. *Nature*, **461**, 1071–1078.
2. Kupiec,M. (2000) Damage-induced recombination in the yeast *Saccharomyces cerevisiae*. *Mutat. Res.*, **451**, 91–105.
3. Thoma,F. (2005) Repair of UV lesions in nucleosomes—intrinsic properties and remodeling. *DNA Repair (Amst)*, **4**, 855–869.
4. Friedberg,E.C., Walker,G.C., Siede,W., Wood,R.D., Schultz,R.A. and Ellenberger,T. (2006) *DNA Repair and Mutagenesis*, 2nd edn. ASM Press, Washington, DC.
5. Prakash,S. and Prakash,L. (2000) Nucleotide excision repair in yeast. *Mutat. Res.*, **451**, 13–24.
6. Kadyk,L.C. and Hartwell,L.H. (1993) Replication-dependent sister chromatid recombination in rad1 mutants of *Saccharomyces cerevisiae*. *Genetics*, **133**, 469–487.
7. Gangavarapu,V., Prakash,S. and Prakash,L. (2007) Requirement of *RAD52* group genes for postreplication repair of UV-damaged DNA in saccharomyces cerevisiae. *Mol. Cell. Biol.*, **27**, 7758–7764.
8. Aboussekhra,A. and Al-Sharif,I.S. (2005) Homologous recombination is involved in transcription-coupled repair of UV damage in *Saccharomyces cerevisiae*. *EMBO J.*, **24**, 1999–2010.
9. Dinant,C., Houtsmuller,A.B. and Vermeulen,W. (2008) Chromatin structure and DNA damage repair. *Epigenetics Chromatin*, **1**, doi:10.1186/1756–8935–1–9.
10. van Attikum,H. and Gasser,S.M. (2005) The histone code at DNA breaks: a guide to repair? *Nat. Rev. Mol. Cell Biol.*, **6**, 757–765.
11. Bostelman,L.J., Keller,A.M., Albrecht,A.M., Arat,A. and Thompson,J.S. (2007) Methylation of histone H3 lysine-79 by Dot1p plays multiple roles in the response to UV damage in *Saccharomyces cerevisiae*. *DNA Repair (Amst.)*, **6**, 383–395.
12. Evans,M.L., Bostelman,L.J., Albrecht,A.M., Keller,A.M., Strande,N.T. and Thompson,J.S. (2008) UV sensitive mutations in

histone H3 in *Saccharomyces cerevisiae* that alter specific K79 methylation states genetically act through distinct DNA repair pathways. *Curr. Genet.*, **53**, 259–274.

13. Conde,F. and San-Segundo,P.A. (2008) Role of Dot1 in the response to alkylating DNA damage in *Saccharomyces cerevisiae*: regulation of DNA damage tolerance by the error-prone polymerases Polzeta/Rev1. *Genetics*, **179**, 1197–1210.

14. Toh,G.W., O'Shaughnessy,A.M., Jimeno,S., Dobbie,I.M., Grenon,M., Maffini,S., O'Rorke,A. and Lowndes,N.F. (2006) Histone H2A phosphorylation and H3 methylation are required for a novel Rad9 DSB repair function following checkpoint activation. *DNA Repair (Amst.)*, **5**, 693–703.

15. Giannattasio,M., Lazzaro,F., Plevani,P. and Muzi-Falconi,M. (2005) The DNA damage checkpoint response requires histone H2B ubiquitination by Rad6-Bre1 and H3 methylation by Dot1. *J. Biol. Chem.*, **280**, 9879–9886.

16. Wysocki,R., Javaheri,A., Allard,S., Sha,F., Cote,J. and Kron,S.J. (2005) Role of Dot1-dependent histone H3 methylation in G1 and S phase DNA damage checkpoint functions of Rad9. *Mol. Cell. Biol.*, **25**, 8430–8443.

17. Huyen,Y., Zgheib,O., Ditullio,R.A. Jr, Gorgoulis,V.G., Zacharatos,P., Petty,T.J., Sheston,E.A., Mellert,H.S., Stavridi,E.S. and Halazonetis,T.D. (2004) Methylated lysine 79 of histone H3 targets 53BP1 to DNA double-strand breaks. *Nature*, **432**, 406–411.

18. Lazzaro,F., Sapountzi,V., Granata,M., Pellicioli,A., Vaze,M., Haber,J.E., Plevani,P., Lydall,D. and Muzi-Falconi,M. (2008) Histone methyltransferase Dot1 and Rad9 inhibit single-stranded DNA accumulation at DSBs and uncapped telomeres. *EMBO J.*, **27**, 1502–1512.

19. Kim,W., Choi,M. and Kim,J.E. (2014) The histone methyltransferase Dot1/DOT1L as a critical regulator of the cell cycle. *Cell Cycle*, **13**, 726–738.

20. Chaudhuri,S., Wyrick,J.J. and Smerdon,M.J. (2009) Histone H3 Lys79 methylation is required for efficient nucleotide excision repair in a silenced locus of *Saccharomyces cerevisiae*. *Nucleic Acids Res.*, **37**, 1690–1700.

21. Tatum,D. and Li,S. (2011) Evidence that the histone methyltransferase Dot1 mediates global genomic repair by methylating histone H3 on lysine 79. *J. Biol. Chem.*, **286**, 17530–17535.

22. Fink,M., Thompson,J.S. and Thoma,F. (2011) Contributions of histone H3 nucleosome core surface mutations to chromatin structures, silencing and DNA repair. *PLoS One*, **6**, e26210.

23. Game,J.C., Williamson,M.S., Spicakova,T. and Brown,J.M. (2006) The *RAD6/BRE1* histone modification pathway in *Saccharomyces* confers radiation resistance through a *RAD51*-dependent process that is independent of *RAD18*. *Genetics*, **173**, 1951–1968.

24. Conde,F., Refolio,E., Cordon-Preciado,V., Cortes-Ledesma,F., Aragon,L., Aguilera,A. and San-Segundo,P.A. (2009) The Dot1 histone methyltransferase and the Rad9 checkpoint adaptor contribute to cohesin-dependent double-strand break repair by sister chromatid recombination in *Saccharomyces cerevisiae*. *Genetics*, **182**, 437–446.

25. Ng,H.H., Feng,Q., Wang,H., Erdjument-Bromage,H., Tempst,P., Zhang,Y. and Struhl,K. (2002) Lysine methylation within the globular domain of histone H3 by Dot1 is important for telomeric silencing and Sir protein association. *Genes Dev.*, **16**, 1518–1527.

26. van Leeuwen,F., Gafken,P.R. and Gottschling,D.E. (2002) Dot1p modulates silencing in yeast by methylation of the nucleosome core. *Cell*, **109**, 745–756.

27. Ng,H.H., Xu,R.M., Zhang,Y. and Struhl,K. (2002) Ubiquitination of histone H2B by Rad6 is required for efficient Dot1-mediated methylation of histone H3 lysine 79. *J. Biol. Chem.*, **277**, 34655–34657.

28. Sun,Z.W. and Allis,C.D. (2002) Ubiquitination of histone H2B regulates H3 methylation and gene silencing in yeast. *Nature*, **418**, 104–108.

29. Shahbazian,M.D., Zhang,K. and Grunstein,M. (2005) Histone H2B ubiquitylation controls processive methylation but not monomethylation by Dot1 and Set1. *Mol. Cell*, **19**, 271–277.

30. Johnson,R.E., Henderson,S.T., Petes,T.D., Prakash,S., Bankmann,M. and Prakash,L. (1992) *Saccharomyces cerevisiae RAD5*-encoded DNA repair protein contains DNA helicase and zinc-binding sequence motifs and affects the stability of simple repetitive sequences in the genome. *Mol. Cell. Biol.*, **12**, 3807–3818.

31. Brachmann,C.B., Davies,A., Cost,G.J., Caputo,E., Li,J., Hieter,P. and Boeke,J.D. (1998) Designer deletion strains derived from *Saccharomyces cerevisiae* S288C: a useful set of strains and plasmids for PCR-mediated gene disruption and other applications. *Yeast*, **14**, 115–132.

32. Mozlin,A.M., Fung,C.W. and Symington,L.S. (2008) Role of the *Saccharomyces cerevisiae* Rad51 paralogs in sister chromatid recombination. *Genetics*, **178**, 113–126.

33. Pringle,J.R. and Hartwell,L.H. (1981) The *Saccharomyces cerevisiae* cell cycle. In: Strathern,JN, Jones,EW and Broach,JR (eds.) *The Molecular Biology of the Yeast Saccharomyces*. Cold Spring Harbor Laboratory Press, Cold Spring Harbor, NY, pp. 97–142.

34. Lea,D.E. and Coulson,C.A. (1949) The distribution of the numbers of mutants in bacterial populations. *J. Genet.*, **49**, 264–285.

35. Spell,R.M. and Jinks-Robertson,S. (2004) Determination of mitotic recombination rates by fluctuation analysis in *Saccharomyces cerevisiae*. *Methods Mol. Biol.*, **262**, 3–12.

36. Glowczewski,L., Waterborg,J.H. and Berman,J.G. (2004) Yeast chromatin assembly complex 1 protein excludes nonacetylatable forms of histone H4 from chromatin and the nucleus. *Mol. Cell. Biol.*, **24**, 10180–10192.

37. Herskowitz,I. and Jensen,R.E. (1991) Putting the HO gene to work: practical uses for mating-type switching. *Meth. Enzymol.*, **194**, 132–146.

38. Elvers,I., Johansson,F., Groth,P., Erixon,K. and Helleday,T. (2011) UV stalled replication forks restart by re-priming in human fibroblasts. *Nucleic Acids Res.*, **39**, 7049–7057.

39. Fasullo,M. and Sun,M. (2008) UV but not X rays stimulate homologous recombination between sister chromatids and homologs in a *Saccharomyces cerevisiae mec1* (ATR) hypomorphic mutant. *Mutat. Res.*, **648**, 73–81.

40. Friedl,A.A., Liefshitz,B., Steinlauf,R. and Kupiec,M. (2001) Deletion of the *SRS2* gene suppresses elevated recombination and DNA damage sensitivity in *rad5* and *rad18* mutants of *Saccharomyces cerevisiae*. *Mutat. Res.*, **486**, 137–146.

41. Blastyak,A., Pinter,L., Unk,I., Prakash,L., Prakash,S. and Haracska,L. (2007) Yeast Rad5 protein required for postreplication repair has a DNA helicase activity specific for replication fork regression. *Mol. Cell*, **28**, 167–175.

42. Haber,J.E. (2012) Mating-type genes and MAT switching in *Saccharomyces cerevisiae*. *Genetics*, **191**, 33–64.

43. Nakanishi,S., Lee,J.S., Gardner,K.E., Gardner,J.M., Takahashi,Y.H., Chandrasekharan,M.B., Sun,Z.W., Osley,M.A., Strahl,B.D., Jaspersen,S.L. *et al.* (2009) Histone H2BK123 monoubiquitination is the critical determinant for H3K4 and H3K79 trimethylation by COMPASS and Dot1. *J. Cell Biol.*, **186**, 371–377.

44. Siede,W., Friedberg,A.S. and Friedberg,E.C. (1993) *RAD9*-dependent G1 arrest defines a second checkpoint for damaged DNA in the cell cycle of *Saccharomyces cerevisiae*. *Proc. Natl. Acad. Sci. U.S.A.*, **90**, 7985–7989.

45. de la Torre-Ruiz,M.A., Green,C.M. and Lowndes,N.F. (1998) *RAD9* and *RAD24* define two additive, interacting branches of the DNA damage checkpoint pathway in budding yeast normally required for Rad53 modification and activation. *EMBO J.*, **17**, 2687–2698.

46. Schulze,J.M., Jackson,J., Nakanishi,S., Gardner,J.M., Hentrich,T., Haug,J., Johnston,M., Jaspersen,S.L., Kobor,M.S. and Shilatifard,A. (2009) Linking cell cycle to histone modifications: SBF and H2B monoubiquitination machinery and cell-cycle regulation of H3K79 dimethylation. *Mol. Cell*, **35**, 626–641.

47. Game,J.C., Williamson,M.S. and Baccari,C. (2005) X-ray survival characteristics and genetic analysis for nine *Saccharomyces* deletion mutants that show altered radiation sensitivity. *Genetics*, **169**, 51–63.

48. Thompson,J.S., Ling,X. and Grunstein,M. (1994) Histone H3 amino terminus is required for telomeric and silent mating locus repression in yeast. *Nature*, **369**, 245–247.

49. Thompson,J.S., Snow,M.L., Giles,S., McPherson,L.E. and Grunstein,M. (2003) Identification of a functional domain within the essential core of histone H3 that is required for telomeric and HM silencing in *Saccharomyces cerevisiae*. *Genetics*, **163**, 447–452.